ANNUAL REVIEWS

Annual Review of Biophysics

Light Microscopy of Mitochondria at the Nanoscale

Stefan Jakobs,[1,2] Till Stephan,[1,2] Peter Ilgen,[1,2] and Christian Brüser[1,2]

[1]Department of NanoBiophotonics, Max Planck Institute for Biophysical Chemistry, 37077 Göttingen, Germany; email: sjakobs@gwdg.de

[2]Clinic of Neurology, University Medical Center Göttingen, 37075 Göttingen, Germany

Annu. Rev. Biophys. 2020. 49:289–308

First published as a Review in Advance on February 24, 2020

The *Annual Review of Biophysics* is online at biophys.annualreviews.org

https://doi.org/10.1146/annurev-biophys-121219-081550

Keywords

mitochondria, live-cell microscopy, nanoscopy, super-resolution microscopy

Abstract

Mitochondria are essential for eukaryotic life. These double-membrane organelles often form highly dynamic tubular networks interacting with many cellular structures. Their highly convoluted contiguous inner membrane compartmentalizes the organelle, which is crucial for mitochondrial function. Since the diameter of the mitochondrial tubules is generally close to the diffraction limit of light microscopy, it is often challenging, if not impossible, to visualize submitochondrial structures or protein distributions using conventional light microscopy. This renders super-resolution microscopy particularly valuable, and attractive, for studying mitochondria. Super-resolution microscopy encompasses a diverse set of approaches that extend resolution, as well as nanoscopy techniques that can even overcome the diffraction limit. In this review, we provide an overview of recent studies using super-resolution microscopy to investigate mitochondria, discuss the strengths and opportunities of the various methods in addressing specific questions in mitochondrial biology, and highlight potential future developments.

Contents

INTRODUCTION 290
Super-Resolution Microscopy, Nanoscopy, and Extended-Resolution Microscopy 291
Improving the Resolution in Far-Field Light Microscopy 292
MITOCHONDRIA AS TARGETS TO EVALUATE THE RESOLVING POWER OF DIFFERENT SUPER-RESOLUTION MICROSCOPY TECHNIQUES 293
MITOCHONDRIAL ARCHITECTURE 294
Protein Distributions within the Inner Membrane 294
Mitochondrial Contact Site and Cristae Organizing System 296
Outer Membrane Proteins 296
Mitochondrial Outer Membrane Permeabilization in Apoptosis 297
Mitochondrial Dynamics and Interactions with Other Cellular Compartments 298
Mitochondrial Nucleoids 299
DIFFERENT METHODS FOR DIFFERENT QUESTIONS 300

INTRODUCTION

Mitochondria, ancient double-membrane organelles, are essential for eukaryotic life (112). They are the powerhouses of the cell, as they harbor the oxidative phosphorylation (OXPHOS) system that synthesizes the vast majority of the ATP required by cellular processes. Besides this, they have a multitude of other cellular functions, including iron–sulfur cluster synthesis, β-oxidation of fatty acids, and biosynthesis of heme and of several phospholipids and other metabolites. Mitochondria also play a key role in apoptosis, and they participate in developmental processes and aging. Indeed, there is increasing evidence that numerous devastating human diseases are associated with mitochondrial dysfunctions (97).

In many cell types, mitochondria form loose and dynamic networks of tubules that constantly move, fuse, and divide (7, 96, 141). These organelles exhibit a smooth outer membrane and a highly folded inner membrane (43, 99, 124). The mitochondrial outer membrane primarily harbors the machinery that is required for communication and physical interaction with other cellular structures. The contiguous inner membrane can be structurally and functionally subdivided into at least two domains, namely, the inner boundary membrane, which parallels the outer membrane, and invaginations of varying shapes, termed cristae (28, 135, 140, 146, 150). The inner boundary membrane and crista membranes are connected by crista junctions, narrow tubules or slits that presumably act as selective barriers for proteins, lipids, and metabolites moving in and out of the crista membrane or the crista lumen (83). The intricate architecture of the inner membrane is crucial for proper function of these organelles in cellular metabolism and apoptosis.

The unique membrane architecture of mitochondria was discovered in the 1950s using transmission electron microscopy, which was at the time a new technology enabling insights into cell biology (99, 124) (**Figure 1**). Subsequently, it took more than half a century to develop another technology, namely, super-resolution microscopy (60, 110, 122), facilitating nanoscale resolution in optical microscopy, as well. As a consequence of this technological advance, researchers can now observe mitochondrial cristae even in living cells (**Figure 1**).

OXPHOS: oxidative phosphorylation

Indeed, mitochondria are challenging objects for optical microscopy, not only because they are very dynamic and sensitive against many stresses in living cells, but also because they are small.

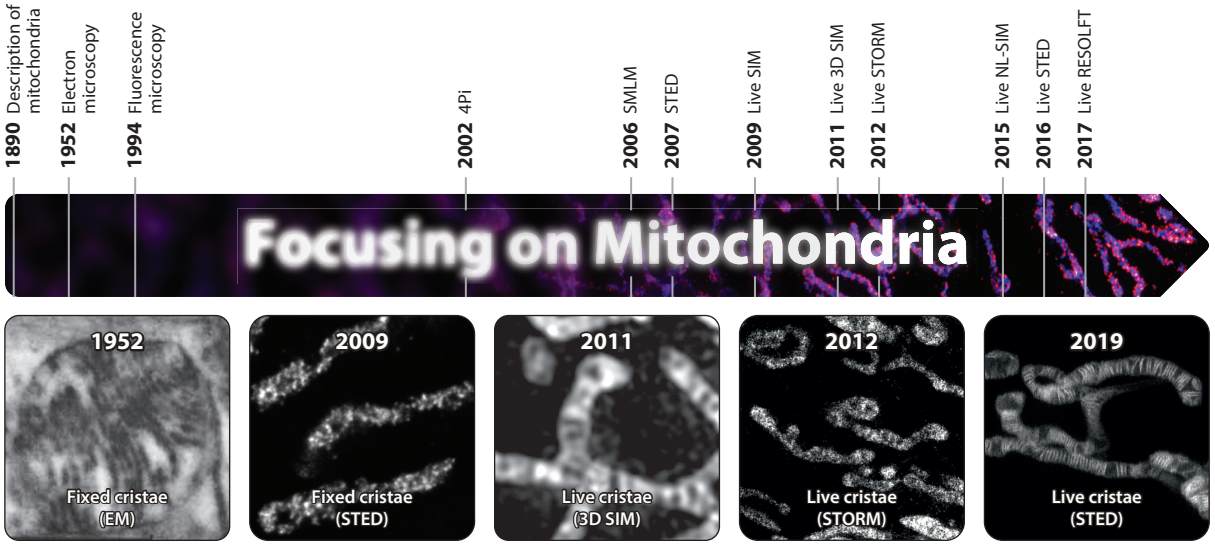

Figure 1

Mitochondria in the focus of microscopy. Highlighted are important milestones for visualization of mitochondria. The years in which certain imaging methods were first used to visualize mitochondria are given. The images show (*from left to right*): one of the first images of cristae recorded by EM (panel adapted with permission from Reference 99); the first light microscopy image of fixed cristae taken by isoSTED nanoscopy (panel adapted with permission from Reference 115); the first visualization of mitochondrial inner membrane structures in living cells by 3D SIM (panel adapted with permission from Reference 24); the first live-cell SMLM of the mitochondrial inner membrane (panel adapted with permission from Reference 121); and one of the first images of individual mitochondrial cristae recorded in living cells using STED nanoscopy (panel adapted with permission from Reference 126). Abbreviations: EM, electron microscopy; NL-SIM, nonlinear structured illumination microscopy; RESOLFT, reversible saturable/switchable optical linear (fluorescence) transitions; SIM, structured illumination microscopy; SMLM, single-molecule localization microscopy; STED, stimulated emission depletion; STORM, stochastic optical reconstruction microscopy.

Although the mitochondrial tubules can be several μm long, their diameter is typically between 200 and 700 nm, which is around the diffraction limit that restricts the attainable resolution in classical (fluorescence) microscopy (1, 9). Thus, with classical optical microscopy, it is always challenging, often even impossible, to visualize submitochondrial structures. This review provides an overview of recent developments in the use of super-resolution microscopy to study mitochondria on the nanoscale.

Super-Resolution Microscopy, Nanoscopy, and Extended-Resolution Microscopy

The terms super-resolution microscopy and nanoscopy are sometimes used synonymously; in other contexts, distinctions between them are made. In this review, we use these terms in the following way: Nanoscopy is strictly used for techniques that fundamentally overcome the diffraction barrier. This includes, among others, approaches such as (fluorescence) photo-activated localization microscopy [(f)PALM] (8, 49), stochastic optical reconstruction microscopy (STORM) (109), points accumulation for imaging in nanoscale topography (PAINT) nanoscopy (119), nonlinear structured illumination microscopy (NL-SIM) (40), reversible saturable/switchable optical linear (fluorescence) transitions (RESOLFT) nanoscopy (47, 51), and stimulated emission depletion (STED) nanoscopy (48, 66). We use the term extended-resolution microscopy (42) to refer to approaches that improve the spatial resolution, compared to conventional confocal or widefield

Nanoscopy: super-resolution microscopy techniques that overcome the diffraction limit

SIM: structured illumination microscopy

RESOLFT: reversible saturable/switchable optical linear (fluorescence) transitions

STED: stimulated emission depletion

fluorescence microscopy, but that do not overcome the diffraction barrier. These methods typically attain a lateral resolution of approximately 100 nm. Thus, the terms extended-resolution microscopy and nanoscopy are nonoverlapping. Examples of extended-resolution microscopy include linear SIM (39), image scanning microscopy (ISM)/AiryScan microscopy (89, 120), lattice light-sheet microscopy (15), super-resolution optical fluctuation imaging (SOFI) (19), and many others, including further fluctuation-based methods and computer-vision-based methods (for an overview, see 113, 134). In this review, we use the term super-resolution microscopy as a general term for extended-resolution microscopy and nanoscopy.

In addition to the methods improving the optical resolution, the recently developed expansion microscopy circumvents the problem of limited spatial resolution by physically increasing the size of the sample (16, 139). It thus achieves a practical resolution in the nanoscopy regime. Inevitably, this method is restricted to fixed specimens. Indeed, mitochondria were among the first organelles analyzed with expansion microscopy, which achieved detailed imaging of membrane protein distributions and cristae structures (30). Still, to our knowledge, expansion microscopy has not yet been used to address questions of mitochondrial biology. Consequently, expansion microscopy is not covered in this review.

Extended-resolution microscopy: super-resolution microscopy techniques that can achieve an optical resolution significantly higher (typically approximately twofold) than attainable in conventional confocal or widefield microscopy but that are still diffraction limited

ISM: image scanning microscopy; also referred to as AiryScan microscopy

Improving the Resolution in Far-Field Light Microscopy

In 1873, Ernst Abbe (1) postulated that the attainable spatial resolution of light microscopy is fundamentally limited. He showed that, due to diffraction, visible light cannot be focused into an infinitesimal small focal area, but only to a spot of approximately 200 nm width in lateral dimensions and approximately 500 nm length along the z axis. As a result, fluorophores within such a diffraction-limited focal spot will all be excited and detected together and are therefore inseparable in conventional light microscopy. Abbe's discovery proved to be correct. However, it holds true only under the conditions met by conventional (fluorescence) light microscopy (42). Over the past two decades, several novel microscopy approaches have been implemented to extend the attainable resolution and even to shatter this resolution limit.

Extending the resolution. The super-resolution methods that enhance the resolution compared to the diffraction limit but do not overcome the barrier make up a diverse set of techniques based on widefield, total internal reflection fluorescence (TIRF), or confocal microscopy (for an overview on these methods, see 113). For imaging mitochondria, SIM and ISM seem to be the most popular microscopy approaches with extended resolution. SIM relies on interference-based periodic light patterns that are projected onto the sample. In SIM, after several images for different positions and orientations of the excitation pattern are recorded, a final image with approximately doubled resolution is calculated by applying a reconstruction algorithm (39, 41, 71). SIM is related to ISM (or AiryScan microscopy), which uses a similar physical principle to increase the resolution in a beam scanning microscope (for a detailed review, see 33). In ISM, an excitation focus is scanned across the specimen, and the fluorescence is recorded by a multipixel detector array (for example, a camera) in the widefield detection mode. Subsequently, from the many images, each taken at an individual scan position, a final image is calculated. Also, ISM can nearly double the resolution.

Compared to nanoscopy, these extended-resolution microscopies attain only a relatively modest spatial resolution but generally also require only modest light powers and provide fast recording times, so that they are often considered to be rather benign to living cells and are particularly useful for live-cell imaging approaches. However, most extended-resolution microscopy methods, including SIM, require mathematical postprocessing, which demands significant expertise to detect and counteract reconstruction artifacts (18, 113).

Overcoming the diffraction limit. The fact that all fluorophores in a diffraction-limited volume are excited together, and therefore fluoresce together, ultimately limits the resolution of conventional fluorescence microscopy. The key to fundamentally overcoming the diffraction limit is to distinguish fluorophores residing in a diffraction-limited volume by keeping them in separable states (47, 48). To this end, molecules are switched between two states, typically a fluorescent on- and a nonfluorescent off-state. Most approaches transfer the majority of the fluorophores in a diffraction-limited volume into the off-state and record few or even a single molecule at a time. This can be achieved by two families of approaches, namely, coordinate-targeted nanoscopy and coordinate-stochastic nanoscopy. Coordinate-targeted nanoscopy techniques are scanning approaches, with STED nanoscopy (48, 66), RESOLFT nanoscopy (11, 35, 51), and the related NL-SIM (40, 79) being the most prominent methods in this category. In this case, the fluorophores are reversibly driven by light between two states. In STED and RESOLFT nanoscopy, a light pattern defining one minimum or multiple minima is used to define subdiffraction regions at which no off-switching occurs, so that the fluorophores can fluoresce only in these regions. In most STED and RESOLFT microscopes, a single minimum, or zero, is generated by a focal spot in the shape of a doughnut. This minimum is scanned across the specimen to generate an image with subdiffraction resolution. The attainable resolution depends on the geometry of the minima and the efficiency of the off-switching process and can therefore be adjusted to the imaging needs. In cellular samples, the attainable resolution is typically between 30 and 50 nm (110). Unlike NL-SIM, which relies on widefield detection, beam-scanning STED and RESOLFT nanoscopy require no additional computational efforts to reconstruct the final images.

SMLM: single-molecule localization microscopy

Coordinate-stochastic nanoscopy methods, often also called single-molecule localization microscopy (SMLM), such as (f)PALM (8, 49), STORM (109), PAINT (119), or one of the related approaches (6, 113, 122), are widefield approaches that rely on the localization of individual molecules that have been stochastically turned into a fluorescent on-state. When isolated in space, the positions of single fluorophores can be determined with precision in the nanometer range. To obtain an image reflecting the distribution of all fluorophores, the process of stochastically switching molecules in the on-state and subsequently switching them off (or bleaching them) has to be iterated numerous times, until enough localization events have been determined to reconstruct an image.

MITOCHONDRIA AS TARGETS TO EVALUATE THE RESOLVING POWER OF DIFFERENT SUPER-RESOLUTION MICROSCOPY TECHNIQUES

Fluorescently labeled cellular structures, notably microtubules and nuclear pores, because of their constant size, geometry, and brightness after labeling, are often-used targets to evaluate the potential and limitations of various fluorescence microscopy methods. Likewise, mitochondria have been used frequently as targets to evaluate microscopy techniques; they often served to facilitate analysis of different characteristics of an imaging scheme because of their complex architecture, structural heterogeneity, and dynamics. Due to their sensitivity against photostress, they are also good targets for evaluating the phototoxicity of a given method.

Already in the early 2000s, it was shown that 4Pi-microscopy, which increases the resolution along the axial axis to approximately 100 nm, enabled a better representation of the complex mitochondrial network in living and fixed cells than was previously possible (20, 22, 36). Similarly, early demonstrations of SIM relied on the imaging of mitochondria (50). Introducing 3D SIM, Mats Gustafsson and colleagues (118) were the first to show mitochondrial substructures that were reminiscent of cristae in living HeLa cells (**Figure 1**). This approach was later extended

to dual-color 3D recordings (24), and with improved data processing, even single cristae could be visualized with an impressive temporal resolution (56). Numerous other studies reporting on developments in SIM and related approaches relied on imaging the dynamics of mitochondria labeled either with dyes or fluorescent proteins (17, 37, 79, 81).

TOM: translocase of the mitochondrial outer membrane

The first nanoscopy images of chemically fixed mitochondria were reported in the study introducing PALM (8), which relied on the photoconvertible protein mEosFP that was targeted to the mitochondrial matrix. Most subsequent studies using SMLM approaches to visualize mitochondrial proteins also recorded chemically fixed samples (54, 67, 133). Notable exceptions relied on the use of several different MitoTracker dyes, which were shown to be live-cell-compatible photoswitchable membrane probes (**Figure 1**) (121), as well as on a photoactivatable ligand of the Halo-tag (26). Recently, mitochondria, even in thick fixed tissues, have been used as targets for studies relying on PAINT nanoscopy (101, 116).

Also, STED nanoscopy was used early on to visualize mitochondrial proteins. The first dual-color STED study reported on the distribution of the translocase of the outer membrane (TOM) complex (21). Numerous studies followed (95, 147), including the first visualization of (chemically fixed) cristae using isoSTED nanoscopy (115) (**Figure 1**), the visualization of mitochondria in bio-banked human tissues (58), and live-cell recordings of mitochondria (10). Recently, the visualization of single cristae in living cells was reported using STED nanoscopy relying on a SNAP-tag fusion protein (126) (**Figure 1**) or an inner-membrane-specific fluorescent probe (138).

The development of resolution-extended microscopy and diffraction-unlimited nanoscopy over the past two decades allowed researchers to address questions the answers to which were previously just out of reach. In the following sections, we discuss some recent studies covering topics of mitochondrial biology that benefited from super-resolution microscopy. Inescapably, given the rapid growth of the field, this snapshot represents a selection of studies that is by no means comprehensive.

MITOCHONDRIAL ARCHITECTURE

Protein Distributions within the Inner Membrane

The intricate fold of the inner membrane early on provoked the idea that the crista membranes and the inner boundary membrane have not only different functions, but also different protein compositions. Initially, such different protein localizations were experimentally demonstrated by immunogold electron microscopy (32, 135) and by the use of conventional light microscopy on genetically enlarged mitochondria (146). These approaches were also used to demonstrate that proteins move in and out of the crista membrane depending on the cellular conditions (128, 130, 135). Several studies using various forms of super-resolution microscopy have confirmed the existence of heterogeneous protein distributions within the inner membrane (23, 67). Accordingly, single-molecule tracking of inner membrane proteins suggested that individual cristae represent diffusion-restricting microcompartments (3) (**Figure 2*a***). A recent study suggested that individual cristae within the same mitochondrion exhibit different membrane potentials, further supporting the view that crista junctions might represent diffusion barriers (84, 143).

Examples of the spatial segregation of protein distributions and functions within the inner membrane are uncoupling protein 4 (UCP4) and the F_1F_O-ATP synthase, both of which can dissipate the proton gradient across the inner membrane. dSTORM revealed that UCP4 and F_1F_O-ATP synthase are spatially separated to the inner boundary membrane and to the crista membranes, respectively (67). This spatial separation to different domains likely prevents UCP4 from uncoupling OXPHOS from the F_1F_O-ATP synthase–mediated proton pumping under normal cellular conditions; UCP4 might only lower the proton motive force if it exceeds a potentially damaging threshold.

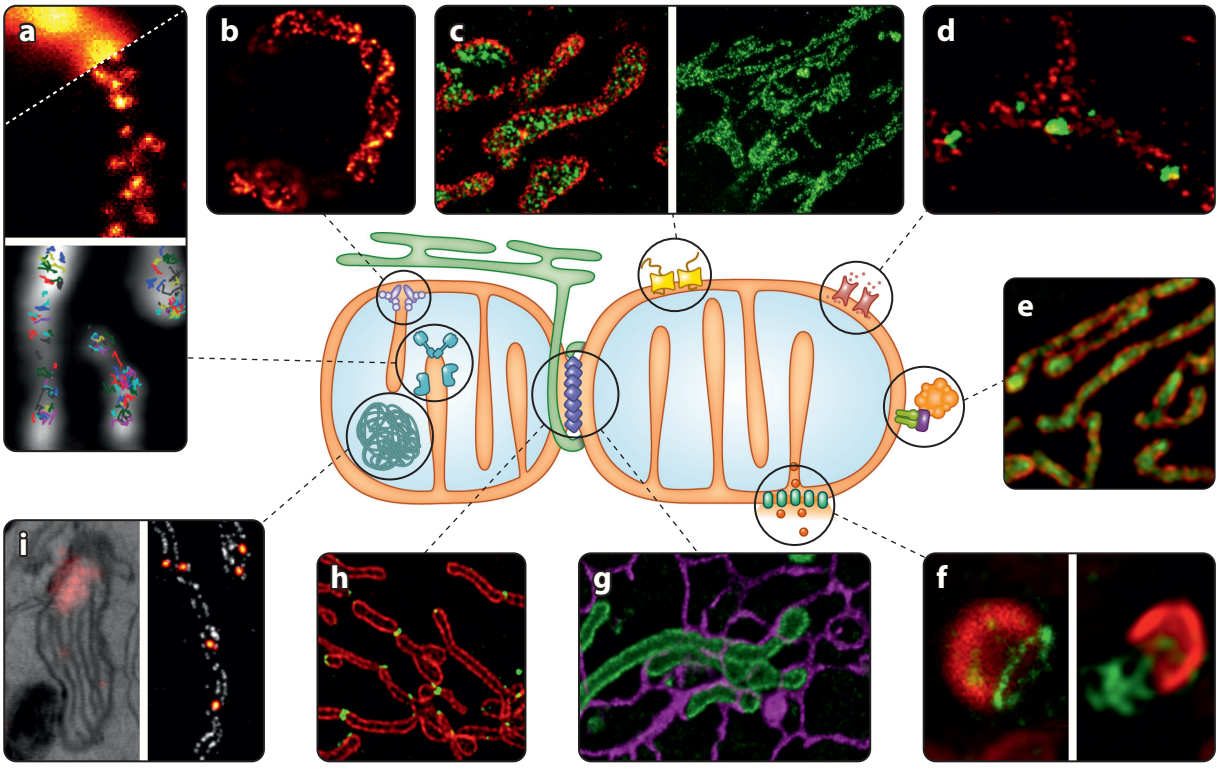

Figure 2

Super-resolution microscopy to address questions of mitochondrial biology. (*a*) OXPHOS. (*Top*) Distribution of assembly factors recorded with STED nanoscopy. Panel adapted with permission from Reference 129. (*Bottom*) Tracking of single OXPHOS subunits using SMLM. Panel adapted with permission from Reference 3. (*b*) Localization of the MICOS subunit Mic60 in a yeast cell, revealed by STED nanoscopy. Panel adapted with permission from Reference 127. (*c*) TOM complex in the outer membrane recorded with DNA-PAINT nanoscopy (*left*, TOM complex in red) (subpanel adapted with permission from Reference 116) and STED nanoscopy (*right*) (subpanel adapted with permission from Reference 147). (*d*) Differential distributions of the three human hVDAC (mitochondrial porin) isoforms in the outer membrane of human mitochondria (STED nanoscopy, hVDAC in green). Panel adapted with permission from Reference 95. (*e*) Sub-mitochondrial localization of PINK1 (*green*) shown by 3D-SIM. Panel adapted with permission from Reference 23. (*f*) Apoptosis. (*Left*) Several proapoptotic BAX proteins (*green*) form ring-like structures in the outer membrane that may act as pores (STED nanoscopy). Panel adapted with permission from Reference 34. (*Right*) During later steps of apoptosis, these large BAX assemblies facilitate the herniation of the inner membrane and release of mtDNA (*green*), as shown by 3D-SIM. Panel adapted with permission from Reference 86. (*g*) Interactions between mitochondria (*green*) and the ER (*purple*) in living cells, recorded by STED nanoscopy. Panel adapted with permission from Reference 10. (*h*) Spatial dynamics of the dynamin-like GTPase DRP1 (*green*), which is essential for mitochondrial fission, visualized by 3D-SIM. Panel adapted with permission from Reference 61. (*i*) Nucleoids, analyzed with correlative PALM and EM (*left*) (subpanel adapted with permission from Reference 68) and with STED nanoscopy (*right*, nucleoids in fire) (C. Brüser and S. Jakobs, unpublished). Abbreviations: BAX, Bcl-2-associated X protein; EM, electron microscopy; ER, endoplasmic reticulum; hVDAC, human voltage-dependent anion channel; MICOS, mitochondrial contact site and cristae organizing system; mtDNA, mitochondrial DNA; OXPHOS, oxidative phosphorylation; PAINT, points accumulation for imaging in nanoscale topography; PALM, photo-activated localization microscopy; SIM, structured illumination microscopy; SMLM, single-molecule localization microscopy; STED, stimulated emission depletion; TOM, translocase of the outer membrane.

OXPHOS is vital for the regeneration of the vast majority of ATP in eukaryotic cells. In higher eukaryotes, it is carried out by five large multisubunit protein complexes. The F_1F_O-ATP synthase is the terminal complex V of the OXPHOS system. In mammals, four of the five OXPHOS complexes are hybrids of subunits encoded in both the nuclear and mitochondrial genomes, and as

such, the assembly of these dual-origin complexes is an enormous logistical challenge for the cell. The fact that the OXPHOS complexes are primarily localized in the crista membranes renders this logistic challenge even more difficult. The assembly of the OXPHOS complexes in yeast mitochondria seems to be rather uniformly distributed along the mitochondrial tubules, as shown by STED nanoscopy (129) (**Figure 2*a***), suggesting that OXPHOS assembly occurs in young as well as in old mitochondria.

MICOS: mitochondrial contact site and cristae organizing system

Still, our understanding of functional domains within the mitochondrial inner membrane is rather rudimentary. Many aspects, such as smaller subdomains, which might be created by proteins such as prohibitins (132), or the role of lipids in the function of this membrane, have been hardly explored.

Mitochondrial Contact Site and Cristae Organizing System

The mitochondrial contact site and cristae organizing system (MICOS) is a large multisubunit protein complex that is essential for the maintenance of the mitochondrial inner membrane architecture and the formation of crista junctions (102, 105). In one of the three studies that first described MICOS (see 45, 53, 136), it was suggested that MICOS may form a filamentous structure within the inner membrane of budding yeast mitochondria (53). Later, several studies investigated the submitochondrial distributions of various MICOS subunits and interacting proteins using nanoscopy, showing that individual MICOS subunits are generally found in well-coordinated, distinct clusters (59, 127, 149).

A core subunit of MICOS is the inner membrane–spanning protein Mic60. Initially, it was reported that, in mammalian cells, Mic60 clusters are distributed along two opposite sides (or distribution bands) of the mitochondria (59). In a subsequent study, it was found that these distribution bands can also be twisted, resulting in a helical arrangement of Mic60 clusters (127) (**Figure 2*b***). Since Mic60 is enriched at the crista junctions (45, 59, 103), these findings suggested that the cristae can also adapt a helical arrangement. Indeed, focused ion beam scanning electron microscopy (FIB-SEM) revealed that, in yeast, the twisting of the opposite distribution bands is echoed by the folding of the inner membrane such that the cristae often seemed to adopt a propeller-like arrangement (127). Intriguingly, spiral-like cristae have also been reported in mitochondria from *Drosophila* (62). Several other Mic60-interacting proteins in the mitochondrial inner and outer membranes seemed to be arranged in a similar patterned manner (127, 149). Based on these observations, it has been speculated that Mic60 is part of a multiprotein interaction network that exhibits a heterogeneous composition (53, 127) and that it is vital for the architecture of the mitochondria, as it might scaffold the organelle. Nanoscopy will undoubtedly facilitate the further investigation of this proposed structure.

Outer Membrane Proteins

The mitochondrial outer membrane contains numerous transporters and channels, most of which are so abundant that their distributions cannot be resolved with diffraction-limited microscopy. The TOM complex is the primary entry gate for nuclear-encoded proteins into the mitochondria. Several studies reported on the clustering of the TOM complexes in the membrane (21, 30, 54, 98, 114, 116) (**Figure 2*c***). STED nanoscopy revealed that, in multiple human cell lines, the antibody-decorated TOM clusters have a diameter of approximately 70 nm, suggesting an actual diameter of the clusters of approximately 40 nm (147) (**Figure 2*c***). As this is substantially larger than a single TOM pore, which has a diameter of approximately 15 nm (88), it was concluded that every TOM cluster represents several interacting import pores. An early high-throughput STED

study that analyzed more than 1,000 cells revealed that the nanoscale distribution of these TOM clusters is finely adjusted to the energetic demands of the cell so that cell growth conditions or the microenvironment of a cell in a microcolony influence the density of the TOM cluster distribution (147). Remarkably, even the localization of a mitochondrion in a cell impacts the cluster density. The TOM cluster distribution seems to correlate strongly to the mitochondrial membrane potential, suggesting that the metabolic load of an individual mitochondrion and the number of its TOM import pores are tightly linked (147).

MOMP: mitochondrial outer membrane permeabilization

Another abundant outer membrane protein is the voltage-dependent anion channel (VDAC, also known as mitochondrial porin). In human cells, three human VDAC (hVDAC) isoforms exist (87). A dual-color STED study reported that hVDAC1 and hVDAC2 are localized in distinct domains, whereas hVDAC3 was more uniformly distributed, suggesting that there are functional differences between these three isoforms (95) (**Figure 2*d***).

An example of a protein that exhibits different activities depending on its localization is the mitochondrial kinase PINK1. Using 3D SIM, it has been suggested that, in healthy HeLa mitochondria, a substantial amount of PINK1 is associated with the crista membrane or localized in the crista lumen (23) (**Figure 2*e***). Upon mitochondrial depolarization, PINK1 translocates to the outer membrane. This is presumably a requirement for mitophagy, and the different submitochondrial localizations of PINK1 may act as a molecular switch mediating different functions of this protein.

Mitochondrial Outer Membrane Permeabilization in Apoptosis

Mitochondria-mediated apoptosis is a genetically encoded program leading to cell death (131). It can be elicited by several different stimuli, and throughout the animal kingdom, apoptosis is essential for normal development and tissue homeostasis. Under normal conditions, a cocktail of proapoptotic proteins localized in the mitochondrial intermembrane space is sequestered from the cytosol. Upon induction of apoptosis, a cascade of events cumulates in mitochondrial outer membrane permeabilization (MOMP), resulting in the release of apoptotic proteins, including cytochrome *c* and Smac/DIABLO (63). In the cytosol, these proteins initiate the activation of caspases, thereby triggering the subsequent apoptotic program. This event is considered as the point of no return, and cells undergoing MOMP are destined to die.

The proapoptotic Bcl-2 family proteins BAX (Bcl-2-associated X protein) and BAK (Bcl-2-antagonistic killer) are key players in MOMP. Upon reception of apoptotic stress, BAX and BAK undergo conformational changes and mediate the rupture of the mitochondrial outer membrane. It has been known for decades that, at later stages of the apoptotic process, BAX and BAK form large clusters on the mitochondrial surface (94, 144). However, the actual mechanism of BAX- and BAK-mediated membrane rupture has been controversial. Recently, several studies using various forms of super-resolution microscopy have made important contributions to the understanding of the process (34, 86, 108, 111). Two studies, utilizing dual-color STED (34) and single-color dSTORM/GSDIM (111) of chemically fixed human cells, respectively, demonstrated that BAX proteins form next to large clusters and also much lighter extended oligomers. Often, these oligomers formed ring-like assemblies in the outer membrane, the interiors of which were devoid of outer membrane proteins, strongly suggesting that these ring-like structures represent pores (34) (**Figure 2*f***). Subsequent studies relying on, among others, ISM and SIM revealed that these BAX/BAK ring-like structures can widen into macropores that even allow the herniation of the inner mitochondrial membrane into the cytosol (86, 108). It has been suggested that this process is associated with the release of mitochondrial DNA into the cytosol, triggering the innate immune cGAS/STING pathway, resulting in an inflammatory response (86) (**Figure 2*f***).

Remarkably, inner membrane herniations were reported previously using electron microscopy (117), but their importance has only been widely acknowledged after their visualization with fluorescence microscopy (2).

Mitochondrial Dynamics and Interactions with Other Cellular Compartments

The highly dynamic mitochondrial networks that constantly change their appearance due to fusion and fission processes entertain numerous, often transient, physical interactions with other cellular components, including the actin and the microtubule cytoskeleton, but also with other organelles such as the endoplasmic reticulum (ER), endosomes, and lysosomes (10, 74) (**Figure 2*g***). The sizes of the mitochondria, as well as those of the interacting structures, are in the range of hundreds of nanometers, rather than in the sub-50-nm size regime. Thus, for many questions of mitochondrial dynamics, a large field of view and a high temporal resolution are the pivotal factors, rather than the ultimate optical resolution. Indeed, several studies used SIM variants and other extended-resolution microscopy techniques to obtain insights into mitochondrial dynamics (46, 113) and mitochondria–microtubule (77), mitochondria–actin (61), and mitochondria–purinosome interactions (13).

The dynamin-related GTPase DRP1 is essential for mitochondrial fission (25, 125). DRP1 clusters were visualized using ISM/AiryScan and SIM imaging, showing that some loosely attached DRP1 clusters move along the mitochondrial tubules, whereas other DRP1 clusters are attached to mitochondria and merge, divide, and occasionally move along the organelle with a speed of approximately 50 nm/s (61). 3D SIM imaging suggested that, through a series of merging and reshaping events, mitochondrially bound DRP1 oligomers develop into rings that encircle the mitochondrion (61) (**Figure 2*b***). The findings led to the conclusion that DRP1 is constantly in an equilibrium between the cytosol and the mitochondria, and that several fission factors, including actin filaments, target DRP1 to fission sites (61).

Several studies have shown that mitochondrial fission preferentially occurs at sites where ER tubules encircle mitochondria (69, 70, 90). In addition, contact sites between the ER and the mitochondria are also important for calcium signaling and lipid transfer (29). In many cultured cell lines, the majority of the mitochondria, the ER, and other organelles are found at the basal cell cortex. Grazing incidence SIM (GI-SIM) has been developed to specifically record subcellular dynamics in this region with approximately 100 nm lateral resolution at very high speed (266 frames/s over thousands of time points) (37). A study using GI-SIM showed that ER–mitochondrion contact sites frequently marked mitochondrial constrictions, and fission events usually occurred at these constriction sites. It was also shown that the majority of mitochondrial fusion events (approximately 60%) take place at ER–mitochondrion contact sites. Remarkably, mitochondrial fusions at ER–mitochondrion interaction sites were nearly twice as fast (12.2 s) as fusions without ER involvement (21.9 s), suggesting an even tighter entanglement of mitochondrial and ER dynamics than previously anticipated. The functional connection among the ER, actin filaments, and mitochondrial fission mediated by DRP1 was also investigated by a study that relied on 3D SIM and conventional live-cell imaging (85). The authors demonstrated that a novel isoform of the actin-nucleating protein Spire1 localizes to the outer mitochondrial membrane. This protein interacts with the ER-bound actin polymerase INF2 (inverted formin 2) and thereby links mitochondria to the ER and the actin cytoskeleton, which preconstrict mitochondrial tubules before DRP1 facilitates fission. These recordings, together with numerous other studies (44, 61, 145), further underscore the view that mitochondria are part of a dynamic multi-organelle network within cells, and that they need to be investigated in this context (91). Fast and rather gentle extended-resolution microscopy methods, even if they do not provide the very highest optical resolution, are a very suitable approach in this case.

Nanoscopy further uncovered the interaction among purinosomes, mitochondria, and microtubules (13, 27). Purinosomes are multi-enzyme complexes mediating the de novo synthesis of purine. These are dynamic structures that were shown to partially colocalize with mitochondria in studies relying on 3D STORM. Interestingly, the dysregulation of mitochondrial function and metabolism influenced the number of purinosome-containing cells, suggesting a functional link between mitochondrial function and purinosome formation (27).

Mitochondrial Nucleoids

Mitochondria maintain their own genome with its own genetic code, which is a remnant of their proteobacterial origin (38). Already in the early 1960s, with electron microscopy of chicken tissue sections, an extranuclear DNA molecule with a contour length of 5 μm could be identified, which later proved to be mitochondrial DNA (mtDNA) (92, 93). The mtDNA is tightly packed into nucleoprotein complexes, termed nucleoids, of which up to several thousand copies are found in human cells.

Earlier studies based on conventional light microscopy led to inconsistent estimates regarding the size of nucleoids (52, 100). Likewise, the number of mtDNA molecules within a single nucleoid was unclear, with data suggesting between 2 and 10 mtDNA molecules per single nucleoid (57, 78). When nucleoids came into the focus of super-resolution microscopy in 2011, two independent studies reported their sizes to range between 70 and 110 nm in mammalian cells using STED nanoscopy (73) and iPALM (12). Several studies, including one using correlative 3D super-resolution fluorescence and electron microscopy to investigate the relationship of mitochondrial nucleoids to membranes (68), followed (**Figure 2*i***). STED imaging of hundreds of cells revealed a frequent clustering of nucleoids (**Figure 2*i***). This clustering depends on the cell type and is altered when outer membrane fusion is disrupted (73, 123). With nanoscopy, individual nucleoids, rather than clusters alone, could be resolved, and a substantially higher number of nucleoids per cell than previously reported was recorded. By combining the number of nucleoids per cell with biochemical data, Kukat et al. (73) showed that many nucleoids in human cells contain only a single copy of mtDNA. Based on this conclusion, it has been estimated that a single human mtDNA is decorated with approximately 1,000 mitochondrial transcription factor A (TFAM) molecules. The insight that many nucleoids contain only one mtDNA refutes the hypothesis of dynamic nucleoids that contain several DNA molecules that can be transferred from one nucleoid to another.

Different nanoscopy studies have come to diverse conclusions on the shape of single nucleoids (12, 68, 72, 73). The reported differences on the shape of nucleoids might well be explained by differences in cell type and the functional status of the cell. In fact, variations and adaptations of nucleoid shape might be functionally important, as they might reflect the compaction level and, consequently, gene expression activity (38).

Currently, there is little insight into the regulation of replication and gene expression on the single nucleoid level, although several reports demonstrated nucleoid-to-nucleoid variations (14, 73, 104). The recently described mitochondrial organization of gene expression (MIOREX) complexes contain mitochondrial ribosomes as well as proteins required for mRNA maturation, translation, and decay; thus, the MIOREX complexes might represent large expressosome-like assemblies (64). In yeast, STED nanoscopy revealed that a fraction of the MIOREX complexes colocalize with nucleoids, whereas other nucleoids are apparently not interacting with the MIOREX complexes, further supporting the concept of nucleoid heterogeneity.

Approximately 25% of the mitochondrial proteome is involved in gene expression. Currently, the spatial organization of these factors within mitochondria is largely unknown, rendering this a large and still mostly unexplored field.

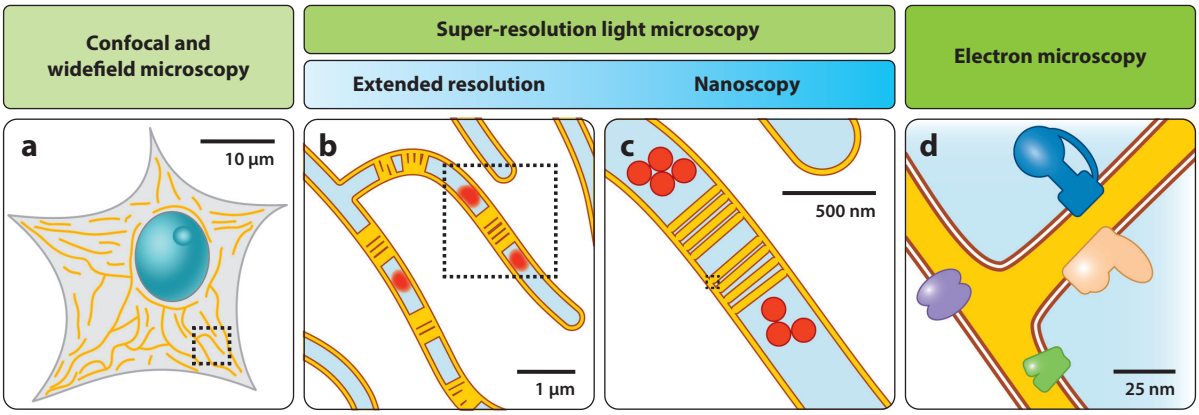

Figure 3

Imaging mitochondria across scales. (*a*) Diffraction-limited microscopy (confocal or widefield microscopy). Overall mitochondrial morphology and network dynamics can be visualized. There is only limited information on submitochondrial protein distributions. (*b*) Extended-resolution microscopy (diffraction-limited super-resolution microscopy). Network dynamics and some inner mitochondrial dynamics can be visualized. Groups of cristae and, under some conditions, single cristae are visible. Mitochondrial subcompartments can be analyzed. (*c*) Nanoscopy (diffraction-unlimited super-resolution microscopy). Detailed submitochondrial protein distributions and individual cristae can be resolved. (*d*) Electron microscopy. Precise membrane architecture and lipid bilayers are resolved. With specific approaches, protein distributions and even protein structures can be determined.

DIFFERENT METHODS FOR DIFFERENT QUESTIONS

As super-resolution microscopy is used to address issues ranging from mitochondrial protein distributions on the nanoscale in fixed cells to network dynamics with very high temporal resolution, it is evident that no single method can serve all purposes (**Figure 3**). The choice of the imaging method will depend on the required temporal and spatial distribution, the specimen, the preferred labeling approach, and whether live or chemically fixed cells are to be recorded (for detailed reviews comparing different super-resolution approaches, see 110, 113, 134).

In the published studies reporting on submitochondrial structures in living cells, STED nanoscopy excels in terms of spatial resolution, whereas SIM shows its full potential when high temporal resolution in combination with a large field of view is required. For example, the SIM images of COS-7 cells labeled with MitoTracker Green (56) (**Figure 4*a***) or MCC13 cells expressing the outer-membrane marker mEmerald-TOM20 (98) (**Figure 4*d***) demonstrate the strength of the approach in recording large fields of view at an extended resolution. In comparison, the STED image of a living HeLa cell expressing a SNAP-tag fusion protein targeted to the crista membranes (126) (**Figure 4*c***) was recorded on a rather small field of view (to ensure a sufficiently high temporal resolution) with a spatial resolution of approximately 50 nm, facilitating a significantly clearer view of individual cristae. Although SMLM has mostly been performed on fixed mitochondria, Shim et al. (121) demonstrated time-lapse STORM images of BS-C-1 cells labeled with MitoTracker Red, which accumulates on the inner membrane. Their recordings revealed thin, extended tubular intermediates connecting neighboring mitochondria both prior to fission and after fusion (**Figure 4*b***). Interestingly, the authors report that tightly packed cristae were better resolved after chemical fixation (121).

A range of different stresses can elicit excessive mitochondrial fission or, occasionally, mitochondrial fusion, resulting in aberrant network morphologies. Therefore, live-cell recordings of mitochondria require care to avoid perturbations of the environmental conditions, notably of the growth medium and the temperature. Likewise, protein tagging and/or protein overexpression

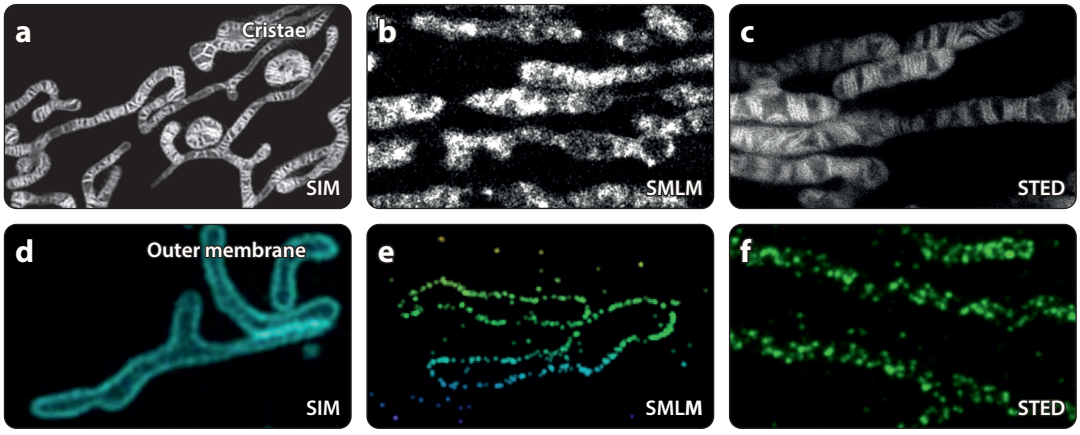

Figure 4

Cristae and TOM complexes recorded with different super-resolution microscopy techniques. (*a–c*) Mitochondrial cristae recorded in living human cells with (*a*) Hessian SIM (panel adapted with permission from Reference 56), (*b*) SMLM (STORM) (panel adapted with permission from Reference 121), (*c*) STED nanoscopy (panel adapted with permission from Reference 126). For SIM and STORM, the cristae were labeled with different MitoTracker dyes. For STED nanoscopy, cells expressing a COX8A-SNAP-tag fusion protein were labeled with a silicone rhodamine dye. (*d–f*) The mitochondrial outer membrane proteins TOM20 or TOM22 were imaged in human cell lines with (*d*) SIM (panel adapted with permission from Reference 98), (*e*) SMLM (4PiSMSN) (panel adapted with permission from Reference 55), and (*f*) STED nanoscopy (panel adapted with permission from Reference 127). For 4PiSMSN and STED nanoscopy, fixed cells were decorated with antibodies against TOM20 (4PiSMSN) or TOM22 (STED nanoscopy). SIM was performed on living cells expressing a TOM20-mEmerald fusion protein. Abbreviations: SIM, structured illumination microscopy; SMLM, single-molecule localization microscopy; SMSN, single-molecule switching nanoscopy; STED, stimulated emission depletion; STORM, stochastic optical reconstruction microscopy; TOM, translocase of the outer membrane.

can interfere with mitochondrial function or architecture, requiring rigorous control experiments (31, 106). In particular, in super-resolution microscopy, the elevated light intensities imposed on the specimen are a notorious concern (75, 137). Nonetheless, SIM has been used to record thousands of images of mitochondria without obvious phototoxic effects (37). Recently, a detailed study on the phototoxic effects of STED nanoscopy came to the conclusion that, at least for short-term imaging (approximately 10 minutes), living cells can also be imaged by STED nanoscopy without substantial photodamage, although negative long-term effects could not be excluded (65). In this regard, the sensitivity of mitochondria to stresses is simultaneously a blessing and a curse, as damages are readily observable.

In fixed cells, all nanoscopy methods can exploit their full resolution potential, as no constraints with respect to phototoxicity or recording times have to be considered. Unlike extended-resolution methods, nanoscopies like SMLM or STED nanoscopy routinely allow for the visualization of distinct protein clusters. For example, the 4PiSMSN image of a fixed COS-7 cell decorated with antibodies against TOM20 shows a single optical section of a large 3D data set encompassing the entire cell recorded with a 3D resolution of 10–20 nm (55) (**Figure 4*e***). Because of the 3D resolution, the image shows the TOM20 clusters at the rim of the mitochondrial tubules, whereas the 2D STED image (127) (**Figure 4*f***) shows a z-projection of TOM22 clusters of an antibody-decorated mitochondrion from a human dermal fibroblast.

Preparation of cells for fixation, as well as the actual fixation process and the subsequent sample treatment procedures, may damage subcellular structures (80, 107, 142, 148). Likewise, the choice of inadequate binders such as poor antibodies may lead to incomplete decoration of the target structure (4, 76). These challenges are obviously also present for conventional microscopy but are considerably more relevant when cells are imaged at an improved resolution.

MINFLUX: nanoscopy with minimal photon fluxes; currently, this method achieves the highest levels of localization precision of all nanoscopy approaches

The development of photostable dyes that either accumulate in the inner membrane (121, 138) or can be used in combination with self-labeling protein tags such as the SNAP-tag (26, 82, 126) opens up new possibilities for live-cell nanoscopy. However, the choice of usable fluorophores is restricted, as all nanoscopy techniques require special dyes to unlock the full potential of the respective method. In contrast, many extended-resolution microscopy techniques work principally with any fluorescent marker and therefore provide the flexibility to use established dyes or cell lines.

Although with nanoscopy the sub-50-nm regime can be routinely addressed, the ultimate resolution to visualize the mitochondrial membranes or to localize proteins within the organelle is still provided by electron microscopy (**Figure 3**). However, electron microscopy is inescapably limited to fixed cells. MINFLUX nanoscopy (5) provides the resolution required to localize proteins at the scale of single digits of nanometers, even in living cells. To our knowledge, optical methods that address this resolution regime have not yet been used to address biological questions, but we propose that they will become an important part of the method portfolio required to dissect mitochondrial biology on the nanoscale. With increasing resolution, it becomes more difficult to assign a specific fluorescence signal to the overall mitochondrial membrane architecture. Therefore, we also predict that correlative approaches that combine (super-resolution) light microscopy with electron microscopy and other techniques on the same specimen will become increasingly important to investigate the nanoscale architecture of mitochondria.

DISCLOSURE STATEMENT

The authors are not aware of any affiliations, memberships, funding, or financial holdings that might be perceived as affecting the objectivity of this review.

ACKNOWLEDGMENTS

We apologize to the authors of the numerous papers that could not be cited due to space constraints. We thank Jaydev Jethwa for carefully proof reading the manuscript. Part of the work described in this review was supported by Germany's Excellence Strategy EXC 2067/1- 390729940 and ERCAdG 835102, and by the German Research Foundation-funded SFB 1190 (project P01), SFB 1286 (project P05), and FOR2848 (project P04).

LITERATURE CITED

1. Abbe E. 1873. Beiträge zur Theorie des Mikroskops und der mikroskopischen Wahrnehmung. *Arch. Mikrosk. Anat.* 9:413–68
2. Ader NR, Hoffmann PC, Ganeva I, Borgeaud AC, Wang C, et al. 2019. Molecular and topological reorganizations in mitochondrial architecture interplay during Bax-mediated steps of apoptosis. *eLife* 8:e40712
3. Appelhans T, Richter CP, Wilkens V, Hess ST, Piehler J, Busch KB. 2012. Nanoscale organization of mitochondrial microcompartments revealed by combining tracking and localization microscopy. *Nano Lett.* 12:610–16
4. Bachmann M, Fiederling F, Bastmeyer M. 2016. Practical limitations of superresolution imaging due to conventional sample preparation revealed by a direct comparison of CLSM, SIM and dSTORM. *J. Microsc.* 262:306–15
5. Balzarotti F, Eilers Y, Gwosch KC, Gynnå AH, Westphal V, et al. 2017. Nanometer resolution imaging and tracking of fluorescent molecules with minimal photon fluxes. *Science* 355:606–12
6. Baumgart F, Arnold AM, Rossboth BK, Brameshuber M, Schütz GJ. 2018. What we talk about when we talk about nanoclusters. *Methods Appl. Fluoresc.* 7:013001

7. Bereiter-Hahn J, Vöth M. 1994. Dynamics of mitochondria in living cells: shape changes, dislocations, fusion, and fission of mitochondria. *Microsc. Res. Tech.* 27:198–219
8. Betzig E, Patterson GH, Sougrat R, Lindwasser OW, Olenych S, et al. 2006. Imaging intracellular fluorescent proteins at nanometer resolution. *Science* 313:1642–45
9. Born M, Wolf E. 1999. *Principles of Optics*. Cambridge, UK: Cambridge Univ. Press. 7th ed.
10. Bottanelli F, Kromann EB, Allgeyer ES, Erdmann RS, Wood Baguley S, et al. 2016. Two-colour live-cell nanoscale imaging of intracellular targets. *Nat. Commun.* 7:10778
11. Brakemann T, Stiel AC, Weber G, Andresen M, Testa I, et al. 2011. A reversibly photoswitchable GFP-like protein with fluorescence excitation decoupled from switching. *Nat. Biotechnol.* 29:942–47
12. Brown TA, Tkachuk AN, Shtengel G, Kopek BG, Bogenhagen DF, et al. 2011. Superresolution fluorescence imaging of mitochondrial nucleoids reveals their spatial range, limits, and membrane interaction. *Mol. Cell Biol.* 31:4994–5010
13. Chan CY, Pedley AM, Kim D, Xia C, Zhuang X, Benkovic SJ. 2018. Microtubule-directed transport of purine metabolons drives their cytosolic transit to mitochondria. *PNAS* 115:13009–14
14. Chatre L, Ricchetti M. 2013. Large heterogeneity of mitochondrial DNA transcription and initiation of replication exposed by single-cell imaging. *J. Cell Sci.* 126:914–26
15. Chen BC, Legant WR, Wang K, Shao L, Milkie DE, et al. 2014. Lattice light-sheet microscopy: imaging molecules to embryos at high spatiotemporal resolution. *Science* 346:1257998
16. Chen F, Tillberg PW, Boyden ES. 2015. Optical imaging: expansion microscopy. *Science* 347:543–48
17. Chen Y, Liu W, Zhang Z, Zheng C, Huang Y, et al. 2018. Multi-color live-cell super-resolution volume imaging with multi-angle interference microscopy. *Nat. Commun.* 9:4818
18. Demmerle J, Innocent C, North AJ, Ball G, Müller M, et al. 2017. Strategic and practical guidelines for successful structured illumination microscopy. *Nat. Protoc.* 12:988–1010
19. Dertinger T, Colyer R, Iyer G, Weiss S, Enderlein J. 2009. Fast, background-free, 3D super-resolution optical fluctuation imaging (SOFI). *PNAS* 106:22287–92
20. Dlaskova A, Spacek T, Santorova J, Plecita-Hlavata L, Berkova Z, et al. 2010. 4Pi microscopy reveals an impaired three-dimensional mitochondrial network of pancreatic islet beta-cells, an experimental model of type-2 diabetes. *Biochim. Biophys. Acta* 1797:1327–41
21. Donnert G, Keller J, Wurm CA, Rizzoli SO, Westphal V, et al. 2007. Two-color far-field fluorescence nanoscopy. *Biophys. J.* 92:L67–69
22. Egner A, Jakobs S, Hell SW. 2002. Fast 100-nm resolution three-dimensional microscope reveals structural plasticity of mitochondria in live yeast. *PNAS* 99:3370–75
23. Fallaize D, Chin LS, Li L. 2015. Differential submitochondrial localization of PINK1 as a molecular switch for mediating distinct mitochondrial signaling pathways. *Cell Signal.* 27:2543–54
24. Fiolka R, Shao L, Rego EH, Davidson MW, Gustafsson MG. 2012. Time-lapse two-color 3D imaging of live cells with doubled resolution using structured illumination. *PNAS* 109:5311–15
25. Fonseca TB, Sánchez-Guerrero A, Milosevic I, Raimundo N. 2019. Mitochondrial fission requires DRP1 but not dynamins. *Nature* 570:E34–42
26. Frei MS, Hoess P, Lampe M, Nijmeijer B, Kueblbeck M, et al. 2019. Photoactivation of silicon rhodamines via a light-induced protonation. *Nat. Commun.* 10:4580
27. French JB, Jones SA, Deng H, Pedley AM, Kim D, et al. 2016. Spatial colocalization and functional link of purinosomes with mitochondria. *Science* 351:733–37
28. Frey TG, Mannella CA. 2000. The internal structure of mitochondria. *Trends Biochem. Sci.* 25:319–24
29. Friedman JR, Lackner LL, West M, DiBenedetto JR, Nunnari J, Voeltz GK. 2011. ER tubules mark sites of mitochondrial division. *Science* 334:358–62
30. Gambarotto D, Zwettler FU, Le Guennec M, Schmidt-Cernohorska M, Fortun D, et al. 2019. Imaging cellular ultrastructures using expansion microscopy (U-ExM). *Nat. Methods* 16:71–74
31. Gibson TJ, Seiler M, Veitia RA. 2013. The transience of transient overexpression. *Nat. Methods* 10:715–21
32. Gilkerson RW, Selker JML, Capaldi RA. 2003. The cristal membrane of mitochondria is the principal site of oxidative phosphorylation. *FEBS Lett.* 546:355–58
33. Gregor I, Enderlein J. 2019. Image scanning microscopy. *Curr. Opin. Chem. Biol.* 51:74–83

34. Grosse L, Wurm CA, Brüser C, Neumann D, Jans DC, Jakobs S. 2016. Bax assembles into large ring-like structures remodeling the mitochondrial outer membrane in apoptosis. *EMBO J.* 35:402–13
35. Grotjohann T, Testa I, Leutenegger M, Bock H, Urban NT, et al. 2011. Diffraction-unlimited all-optical imaging and writing with a photochromic GFP. *Nature* 478:204–8
36. Gugel H, Bewersdorf J, Jakobs S, Engelhardt J, Storz R, Hell SW. 2004. Cooperative 4Pi excitation and detection yields sevenfold sharper optical sections in live-cell microscopy. *Biophys. J.* 87:4146–52
37. Guo Y, Li D, Zhang S, Yang Y, Liu JJ, et al. 2018. Visualizing intracellular organelle and cytoskeletal interactions at nanoscale resolution on millisecond timescales. *Cell* 175:1430–42.e17
38. Gustafsson CM, Falkenberg M, Larsson NG. 2016. Maintenance and expression of mammalian mitochondrial DNA. *Annu. Rev. Biochem.* 85:133–60
39. Gustafsson MG. 2000. Surpassing the lateral resolution limit by a factor of two using structured illumination microscopy. *J. Microsc.* 198:82–87
40. Gustafsson MG. 2005. Nonlinear structured-illumination microscopy: wide-field fluorescence imaging with theoretically unlimited resolution. *PNAS* 102:13081–86
41. Gustafsson MG, Shao L, Carlton PM, Wang CJ, Golubovskaya IN, et al. 2008. Three-dimensional resolution doubling in wide-field fluorescence microscopy by structured illumination. *Biophys. J.* 94:4957–70
42. Gustafsson MGL. 1999. Extended resolution fluorescence microscopy. *Curr. Opin. Struct. Biol.* 9:627–34
43. Hackenbrock CR. 1968. Chemical and physical fixation of isolated mitochondria in low-energy and high-energy states. *PNAS* 61:598–605
44. Han Y, Li M, Qiu F, Zhang M, Zhang YH. 2017. Cell-permeable organic fluorescent probes for live-cell long-term super-resolution imaging reveal lysosome-mitochondrion interactions. *Nat. Commun.* 8:1307
45. Harner M, Korner C, Walther D, Mokranjac D, Kaesmacher J, et al. 2011. The mitochondrial contact site complex, a determinant of mitochondrial architecture. *EMBO J.* 30:4356–70
46. Heintzmann R, Huser T. 2017. Super-resolution structured illumination microscopy. *Chem. Rev.* 117:13890–908
47. Hell SW, Dyba M, Jakobs S. 2004. Concepts for nanoscale resolution in fluorescence microscopy. *Curr. Opin. Neurobiol.* 14:599–609
48. Hell SW, Wichmann J. 1994. Breaking the diffraction resolution limit by stimulated emission: stimulated-emission-depletion fluorescence microscopy. *Opt. Lett.* 19:780–82
49. Hess ST, Girirajan TP, Mason MD. 2006. Ultra-high resolution imaging by fluorescence photoactivation localization microscopy. *Biophys. J.* 91:4258–72
50. Hirvonen LM, Wicker K, Mandula O, Heintzmann R. 2009. Structured illumination microscopy of a living cell. *Eur. Biophys. J.* 38:807–12
51. Hofmann M, Eggeling C, Jakobs S, Hell SW. 2005. Breaking the diffraction barrier in fluorescence microscopy at low light intensities by using reversibly photoswitchable proteins. *PNAS* 102:17565–69
52. Holt IJ, He J, Mao CC, Boyd-Kirkup JD, Martinsson P, et al. 2007. Mammalian mitochondrial nucleoids: organizing an independently minded genome. *Mitochondrion* 7:311–21
53. Hoppins S, Collins SR, Cassidy-Stone A, Hummel E, Devay RM, et al. 2011. A mitochondrial-focused genetic interaction map reveals a scaffold-like complex required for inner membrane organization in mitochondria. *J. Cell Biol.* 195:323–40
54. Huang B, Jones SA, Brandenburg B, Zhuang X. 2008. Whole-cell 3D STORM reveals interactions between cellular structures with nanometer-scale resolution. *Nat. Methods* 5:1047–52
55. Huang F, Sirinakis G, Allgeyer ES, Schroeder LK, Duim WC, et al. 2016. Ultra-high resolution 3D imaging of whole cells. *Cell* 166:1028–40
56. Huang X, Fan J, Li L, Liu H, Wu R, et al. 2018. Fast, long-term, super-resolution imaging with Hessian structured illumination microscopy. *Nat. Biotechnol.* 36:451–59
57. Iborra FJ, Kimura H, Cook PR. 2004. The functional organization of mitochondrial genomes in human cells. *BMC Biol.* 2:9
58. Ilgen P, Stoldt S, Conradi LC, Wurm CA, Ruschoff J, et al. 2014. STED super-resolution microscopy of clinical paraffin-embedded human rectal cancer tissue. *PLOS ONE* 9:e101563
59. Jans DC, Wurm CA, Riedel D, Wenzel D, Stagge F, et al. 2013. STED super-resolution microscopy reveals an array of MINOS clusters along human mitochondria. *PNAS* 110:8936–41

60. Ji N, Shroff H, Zhong H, Betzig E. 2008. Advances in the speed and resolution of light microscopy. *Curr. Opin. Neurobiol.* 18:605–16
61. Ji WK, Hatch AL, Merrill RA, Strack S, Higgs HN. 2015. Actin filaments target the oligomeric maturation of the dynamin GTPase Drp1 to mitochondrial fission sites. *eLife* 4:e11553
62. Jiang YF, Lin SS, Chen JM, Tsai HZ, Hsieh TS, Fu CY. 2017. Directing the self-assembly of tumour spheroids by bioprinting cellular heterogeneous models with alginate/gelatin hydrogels. *Sci. Rep.* 7:45474
63. Kalkavan H, Green DR. 2018. MOMP, cell suicide as a BCL-2 family business. *Cell Death Differ.* 25:46–55
64. Kehrein K, Schilling R, Möller-Hergt BV, Wurm CA, Jakobs S, et al. 2015. Organization of mitochondrial gene expression in two distinct ribosome-containing assemblies. *Cell Rep.* 10:843–53
65. Kilian N, Goryaynov A, Lessard MD, Hooker G, Toomre D, et al. 2018. Assessing photodamage in live-cell STED microscopy. *Nat. Methods* 15:755–56
66. Klar TA, Jakobs S, Dyba M, Egner A, Hell SW. 2000. Fluorescence microscopy with diffraction resolution barrier broken by stimulated emission. *PNAS* 97:8206–10
67. Klotzsch E, Smorodchenko A, Löfler L, Moldzio R, Parkinson E, et al. 2015. Superresolution microscopy reveals spatial separation of UCP4 and F_0F_1-ATP synthase in neuronal mitochondria. *PNAS* 112:130–35
68. Kopek BG, Shtengel G, Xu CS, Clayton DA, Hess HF. 2012. Correlative 3D superresolution fluorescence and electron microscopy reveal the relationship of mitochondrial nucleoids to membranes. *PNAS* 109:6136–41
69. Korobova F, Gauvin TJ, Higgs HN. 2014. A role for myosin II in mammalian mitochondrial fission. *Curr. Biol.* 24:409–14
70. Korobova F, Ramabhadran V, Higgs HN. 2013. An actin-dependent step in mitochondrial fission mediated by the ER-associated formin INf2. *Science* 339:464–67
71. Kraus F, Miron E, Demmerle J, Chitiashvili T, Budco A, et al. 2017. Quantitative 3D structured illumination microscopy of nuclear structures. *Nat. Protoc.* 12:1011–28
72. Kukat C, Davies KM, Wurm CA, Spåhr H, Bonekamp NA, et al. 2015. Cross-strand binding of TFAM to a single mtDNA molecule forms the mitochondrial nucleoid. *PNAS* 112:11288–93
73. Kukat C, Wurm CA, Spåhr H, Falkenberg M, Larsson NG, Jakobs S. 2011. Super-resolution microscopy reveals that mammalian mitochondrial nucleoids have a uniform size and frequently contain a single copy of mtDNA. *PNAS* 108:13534–39
74. Lackner LL. 2019. The expanding and unexpected functions of mitochondria contact sites. *Trends Cell Biol.* 29:580–90
75. Laissue PP, Alghamdi RA, Tomancak P, Reynaud EG, Shroff H. 2017. Assessing phototoxicity in live fluorescence imaging. *Nat. Methods* 14:657–61
76. Lau L, Lee YL, Sahl SJ, Stearns T, Moerner WE. 2012. STED microscopy with optimized labeling density reveals 9-fold arrangement of a centriole protein. *Biophys. J.* 102:2926–35
77. Lawrence EJ, Boucher E, Mandato CA. 2016. Mitochondria-cytoskeleton associations in mammalian cytokinesis. *Cell Div.* 11:3
78. Legros F, Malka F, Frachon P, Lombès A, Rojo M. 2004. Organization and dynamics of human mitochondrial DNA. *J. Cell Sci.* 117:2653–62
79. Li D, Shao L, Chen BC, Zhang X, Zhang M, et al. 2015. Extended-resolution structured illumination imaging of endocytic and cytoskeletal dynamics. *Science* 349:aab3500
80. Li Y, Almassalha LM, Chandler JE, Zhou X, Stypula-Cyrus YE, et al. 2017. The effects of chemical fixation on the cellular nanostructure. *Exp. Cell Res.* 358:253–59
81. Liu W, Liu Q, Zhang Z, Han Y, Kuang C, et al. 2019. Three-dimensional super-resolution imaging of live whole cells using galvanometer-based structured illumination microscopy. *Opt. Express* 27:7237–48
82. Lukinavicius G, Umezawa K, Olivier N, Honigmann A, Yang G, et al. 2013. A near-infrared fluorophore for live-cell super-resolution microscopy of cellular proteins. *Nat. Chem.* 5:132–39
83. Mannella CA, Marko M, Penczek P, Barnard D, Frank J. 1994. The internal compartmentation of rat-liver mitochondria: tomographic study using the high-voltage transmission electron microscope. *Microsc. Res. Tech.* 27:278–83

84. Mannella CA, Pfeiffer DR, Bradshaw PC, Moraru II, Slepchenko B, et al. 2001. Topology of the mitochondrial inner membrane: dynamics and bioenergetics implications. *IUBMB Life* 52:93–100
85. Manor U, Bartholomew S, Golani G, Christenson E, Kozlov M, et al. 2015. A mitochondria-anchored isoform of the actin-nucleating spire protein regulates mitochondrial division. *eLife* 4:e08828
86. McArthur K, Whitehead LW, Heddleston JM, Li L, Padman BS, et al. 2018. BAK/BAX macropores facilitate mitochondrial herniation and mtDNA efflux during apoptosis. *Science* 359:eaao6047
87. Messina A, Reina S, Guarino F, De Pinto V. 2012. VDAC isoforms in mammals. *Biochim. Biophys. Acta* 1818:1466–76
88. Model K, Meisinger C, Kühlbrandt W. 2008. Cryo-electron microscopy structure of a yeast mitochondrial preprotein translocase. *J. Mol. Biol.* 383:1049–57
89. Müller CB, Enderlein J. 2010. Image scanning microscopy. *Phys. Rev. Lett.* 104:198101
90. Murley A, Lackner LL, Osman C, West M, Voeltz GK, et al. 2013. ER-associated mitochondrial division links the distribution of mitochondria and mitochondrial DNA in yeast. *eLife* 2:e00422
91. Murley A, Nunnari J. 2016. The emerging network of mitochondria-organelle contacts. *Mol. Cell* 61:648–53
92. Nass MM. 1969. Mitochondrial DNA. I. Intramitochondrial distribution and structural relations of single- and double-length circular DNA. *J. Mol. Biol.* 42:521–28
93. Nass MM, Nass S. 1963. Intramitochondrial fibers with DNA characteristics. I. Fixation and electron staining reactions. *J. Cell Biol.* 19:593–611
94. Nechushtan A, Smith CL, Lamensdorf I, Yoon SH, Youle RJ. 2001. Bax and Bak coalesce into novel mitochondria-associated clusters during apoptosis. *J. Cell Biol.* 153:1265–76
95. Neumann D, Bückers J, Kastrup L, Hell SW, Jakobs S. 2010. Two-color STED microscopy reveals different degrees of colocalization between hexokinase-I and the three human VDAC isoforms. *PMC Biophys.* 3:4
96. Nunnari J, Marshall WF, Straight A, Murray A, Sedat JW, Walter P. 1997. Mitochondrial transmission during mating in *Saccharomyces cerevisiae* is determined by mitochondrial fusion and fission and the intramitochondrial segregation of mitochondrial DNA. *Mol. Biol. Cell.* 8:1233–42
97. Nunnari J, Suomalainen A. 2012. Mitochondria: in sickness and in health. *Cell* 148:1145–59
98. Opstad IS, Wolfson DL, Øie CI, Ahluwalia BS. 2018. Multi-color imaging of sub-mitochondrial structures in living cells using structured illumination microscopy. *Nanophotonics* 7:935–47
99. Palade GE. 1952. The fine structure of mitochondria. *Anat. Rec.* 114:427–51
100. Park CB, Larsson NG. 2011. Mitochondrial DNA mutations in disease and aging. *J. Cell Biol.* 193:809–18
101. Park S, Kang W, Kwon YD, Shim J, Kim S, et al. 2018. Superresolution fluorescence microscopy for 3D reconstruction of thick samples. *Mol. Brain* 11:17
102. Pfanner N, van der Laan M, Amati P, Capaldi RA, Caudy AA, et al. 2014. Uniform nomenclature for the mitochondrial contact site and cristae organizing system. *J. Cell Biol.* 204:1083–86
103. Rabl R, Soubannier V, Scholz R, Vogel F, Mendl N, et al. 2009. Formation of cristae and crista junctions in mitochondria depends on antagonism between Fcj1 and Su e/g. *J. Cell Biol.* 185:1047–63
104. Rajala N, Gerhold JM, Martinsson P, Klymov A, Spelbrink JN. 2014. Replication factors transiently associate with mtDNA at the mitochondrial inner membrane to facilitate replication. *Nucleic Acids Res.* 42:952–67
105. Rampelt H, Zerbes RM, van der Laan M, Pfanner N. 2017. Role of the mitochondrial contact site and cristae organizing system in membrane architecture and dynamics. *Biochim. Biophys. Acta* 1864:737–46
106. Ratz M, Testa I, Hell SW, Jakobs S. 2015. CRISPR/Cas9-mediated endogenous protein tagging for RESOLFT super-resolution microscopy of living human cells. *Sci. Rep.* 5:9592
107. Richter KN, Revelo NH, Seitz KJ, Helm MS, Sarkar D, et al. 2018. Glyoxal as an alternative fixative to formaldehyde in immunostaining and super-resolution microscopy. *EMBO J.* 37:139–59
108. Riley JS, Quarato G, Cloix C, Lopez J, O'Prey J, et al. 2018. Mitochondrial inner membrane permeabilisation enables mtDNA release during apoptosis. *EMBO J.* 37:e99238
109. Rust M, Bates M, Zhuang X. 2006. Sub-diffraction-limit imaging by stochastic optical reconstruction microscopy (STORM). *Nat. Methods* 3:793–95

110. Sahl SJ, Hell SW, Jakobs S. 2017. Fluorescence nanoscopy in cell biology. *Nat. Rev. Mol. Cell Biol.* 18:685–701
111. Salvador-Gallego R, Mund M, Cosentino K, Schneider J, Unsay J, et al. 2016. Bax assembly into rings and arcs in apoptotic mitochondria is linked to membrane pores. *EMBO J.* 35:389–401
112. Scheffler IE. 2008. *Mitochondria*. Hoboken, NJ: Wiley. 2nd ed.
113. Schermelleh L, Ferrand A, Huser T, Eggeling C, Sauer M, et al. 2019. Super-resolution microscopy demystified. *Nat. Cell Biol.* 21:72–84
114. Schmidt R, Wurm CA, Jakobs S, Engelhardt J, Egner A, Hell SW. 2008. Spherical nanosized focal spot unravels the interior of cells. *Nat. Methods* 5:539–44
115. Schmidt R, Wurm CA, Punge A, Egner A, Jakobs S, Hell SW. 2009. Mitochondrial cristae revealed with focused light. *Nano Lett.* 9:2508–10
116. Schueder F, Lara-Gutierrez J, Beliveau BJ, Saka SK, Sasaki HM, et al. 2017. Multiplexed 3D super-resolution imaging of whole cells using spinning disk confocal microscopy and DNA-PAINT. *Nat. Commun.* 8:2090
117. Sesso A, Belizario JE, Marques MM, Higuchi ML, Schumacher RI, et al. 2012. Mitochondrial swelling and incipient outer membrane rupture in preapoptotic and apoptotic cells. *Anat. Rec.* 295:1647–59
118. Shao L, Kner P, Rego EH, Gustafsson MG. 2011. Super-resolution 3D microscopy of live whole cells using structured illumination. *Nat. Methods* 8:1044–46
119. Sharonov A, Hochstrasser RM. 2006. Wide-field subdiffraction imaging by accumulated binding of diffusing probes. *PNAS* 103:18911–16
120. Sheppard CJR. 1988. Super-resolution in confocal imaging. *Optik* 80:53–54
121. Shim SH, Xia C, Zhong G, Babcock HP, Vaughan JC, et al. 2012. Super-resolution fluorescence imaging of organelles in live cells with photoswitchable membrane probes. *PNAS* 109:13978–83
122. Sigal YM, Zhou R, Zhuang X. 2018. Visualizing and discovering cellular structures with super-resolution microscopy. *Science* 361:880–87
123. Silva Ramos E, Motori E, Bruser C, Kuhl I, Yeroslaviz A, et al. 2019. Mitochondrial fusion is required for regulation of mitochondrial DNA replication. *PLOS Genet.* 15:e1008085
124. Sjöstrand FS. 1953. Electron microscopy of mitochondria and cytoplasmic double membranes. *Nature* 171:30–32
125. Smirnova E, Griparic L, Shurland DL, van der Bliek AM. 2001. Dynamin-related protein Drp1 is required for mitochondrial division in mammalian cells. *Mol. Biol. Cell* 12:2245–56
126. Stephan T, Roesch A, Riedel D, Jakobs S. 2019. Live-cell STED nanoscopy of mitochondrial cristae. *Sci. Rep.* 9:12419
127. Stoldt S, Stephan T, Jans DC, Brüser C, Lange F, et al. 2019. Mic60 exhibits a coordinated clustered distribution along and across yeast and mammalian mitochondria. *PNAS* 116:9853–58
128. Stoldt S, Wenzel D, Hildenbeutel M, Wurm CA, Herrmann JM, Jakobs S. 2012. The inner-mitochondrial distribution of Oxa1 depends on the growth conditions and on the availability of substrates. *Mol. Biol. Cell* 23:2292–301
129. Stoldt S, Wenzel D, Kehrein K, Riedel D, Ott M, Jakobs S. 2018. Spatial orchestration of mitochondrial translation and OXPHOS complex assembly. *Nat. Cell Biol.* 20:528–34
130. Suppanz IE, Wurm CA, Wenzel D, Jakobs S. 2009. The m-AAA protease processes cytochrome c peroxidase preferentially at the inner boundary membrane of mitochondria. *Mol. Biol. Cell* 20:572–80
131. Tait SW, Green DR. 2010. Mitochondria and cell death: outer membrane permeabilization and beyond. *Nat. Rev. Mol. Cell Biol.* 11:621–32
132. Tatsuta T, Model K, Langer T. 2005. Formation of membrane-bound ring complexes by prohibitins in mitochondria. *Mol. Biol. Cell* 16:248–59
133. van de Linde S, Sauer M, Heilemann M. 2008. Subdiffraction-resolution fluorescence imaging of proteins in the mitochondrial inner membrane with photoswitchable fluorophores. *J. Struct. Biol.* 164:250–54
134. Vangindertael J, Camacho R, Sempels W, Mizuno H, Dedecker P, Janssen KPF. 2018. An introduction to optical super-resolution microscopy for the adventurous biologist. *Methods Appl. Fluoresc.* 6:022003

135. Vogel F, Bornhövd C, Neupert W, Reichert AS. 2006. Dynamic subcompartmentalization of the mitochondrial inner membrane. *J. Cell Biol.* 175:237–47
136. von der Malsburg K, Muller JM, Bohnert M, Oeljeklaus S, Kwiatkowska P, et al. 2011. Dual role of mitofilin in mitochondrial membrane organization and protein biogenesis. *Dev. Cell* 21:694–707
137. Wäldchen S, Lehmann J, Klein T, van de Linde S, Sauer M. 2015. Light-induced cell damage in live-cell super-resolution microscopy. *Sci. Rep.* 5:15348
138. Wang C, Taki M, Sato Y, Tamura Y, Yaginuma H, et al. 2019. A photostable fluorescent marker for the superresolution live imaging of the dynamic structure of the mitochondrial cristae. *PNAS* 116:15817–22
139. Wassie AT, Zhao Y, Boyden ES. 2019. Expansion microscopy: principles and uses in biological research. *Nat. Methods* 16:33–41
140. Werner S, Neupert W. 1972. Functional and biogenetical heterogeneity of the inner membrane of rat-liver mitochondria. *Eur. J. Biochem.* 25:379–96
141. Westermann B. 2010. Mitochondrial fusion and fission in cell life and death. *Nat. Rev. Mol. Cell Biol.* 11:872–84
142. Whelan DR, Bell TD. 2015. Image artifacts in single molecule localization microscopy: why optimization of sample preparation protocols matters. *Sci. Rep.* 5:7924
143. Wolf DM, Segawa M, Kondadi AK, Anand R, Bailey ST, et al. 2019. Individual cristae within the same mitochondrion display different membrane potentials and are functionally independent. *EMBO J.* 38:e101056
144. Wolter KG, Hsu YT, Smith CL, Nechushtan A, Xi XG, Youle RJ. 1997. Movement of Bax from the cytosol to mitochondria during apoptosis. *J. Cell Biol.* 139:1281–92
145. Wong YC, Ysselstein D, Krainc D. 2018. Mitochondria-lysosome contacts regulate mitochondrial fission via RAB7 GTP hydrolysis. *Nature* 554:382–86
146. Wurm CA, Jakobs S. 2006. Differential protein distributions define two sub-compartments of the mitochondrial inner membrane in yeast. *FEBS Lett.* 580:5628–34
147. Wurm CA, Neumann D, Lauterbach MA, Harke B, Egner A, et al. 2011. Nanoscale distribution of mitochondrial import receptor Tom20 is adjusted to cellular conditions and exhibits an inner-cellular gradient. *PNAS* 108:13546–51
148. Wurm CA, Neumann D, Schmidt R, Egner A, Jakobs S. 2010. Sample preparation for STED microscopy. In *Live Cell Imaging: Methods and Protocols*, ed. DB Papkovsky, pp. 185–99. Berlin: Springer
149. Zhou W, Ma D, Sun AX, Tran HD, Ma DL, et al. 2019. PD-linked CHCHD2 mutations impair CHCHD10 and MICOS complex leading to mitochondria dysfunction. *Hum. Mol. Genet.* 28:1100–16
150. Zick M, Rabl R, Reichert AS. 2009. Cristae formation-linking ultrastructure and function of mitochondria. *Biochim. Biophys. Acta* 1793:5–19